# VALIDATION OF A NUMERICAL APPROACH TO THE ANALYSIS OF A LIVE-LINE WORKER EXPOSURE TO THE ELECTRIC FIELD

**W. Krajewski** [*]

Institute of Electrical Engineering, 04-703 Warsaw, Pożaryskiego 28, Poland

**Abstract**—The aim of this paper is to validate a proposed simplified boundary-integral approach (that is called here LEM&BEM) for the analysis of electric field in a live-line-working zone. A human body model of a simplified geometry that is applied to the electric field estimation around the live-line worker is also tested. Numerical results of a more accurate numerical approach, laboratory measurements as well as results of measurements taken on a real tower of HV overhead line are employed for this purpose. The numerical analysis of the electric field distribution in the hot-stick working zone on an anchor tower of 400 kV transmission line is presented to demonstrate the effectiveness of the numerical technique under consideration. The author's own software packages has been applied in computations.

## 1. INTRODUCTION

The electric power industry wishes to avoid loss of supply, for which it receives customer complaints or can be financially penalized. On the other hand, the electricity companies are forced to maintain their electrical equipment on a proper basis.

Due to the risk of electric shock, it is normally necessary for equipment to be isolated from the supply before being worked upon, what is named a planned outage. To avoid the planned outages and to increase the reliability of electric power supply, a technique called live-line working is applied. This technique consists in the maintenance of electrical equipment, often operating at extremely high voltages, while this equipment is still energized.

In general, there are three following methods of live-line working: hot-glove, hot-stick, and bare-hand working.

**Figure 1.** Live-line working on overhead lines. (a) Hot-glove workers on 15 kV line. (b) Hot-stick workers and bare-hand worker on 400 kV transmission line.

- Hot-glove working (Figure 1(a)) is applied for low and medium voltages. To avoid an electric shock, the lineman wears insulating gloves of an appropriate standard. These gloves are often extended to the shoulder to protect the worker's arms. Additional protection can be provided by a rubberised apron, insulated tools such as pliers, etc..

- Hot-stick working is applied for high voltages. The insulating sticks enable the linemen to carry out the work without transgressing a minimum clearance distance from live equipment. Tools, such as hooks or box wrenches are mounted at the end of these sticks. Figure 1(b) presents the hot-stick workers that operate on the cross-arm of the HV tower.

- Bare-hand working is applied for high and extremely high voltages. In this case, the lineman operates most often on an isolated platform or ladder. He can also be suspended from a helicopter or even can sit or stand directly on live conductors. He wears special conducting overall that is connected to the live element near which the work is carried out. This suit acts as a Faraday cage, which equalises the electric potential over the body. In Figure 1(b), the bare-hand worker that seats on a bare conductor near insulators is shown.

Live-line workers are exposed to the electric and magnetic fields of power frequency. These fields should be estimated and analysed for the protection of health and safety of workers. Relatively high strength of these fields appear during bare-hand and hot-stick working. In the first case, as it was mentioned, the worker operates very closely to an energised installation of the high or extremely high voltage. The conductive overall protects him against the influence of the electric field. Unfortunately, this clothing does not protect the lineman against

the penetration of the magnetic field. This field induces eddy-currents in his body. The problem of numerical evaluation of currents induced in the human body due to the external magnetic or electromagnetic fields was investigated, e.g., in papers [1–7], and also reported in previous works by the author [8, 9].

In the case of hot-stick working, the lineman does not wear the conductive suit for the ergonomic reason; therefore, he is exposed to the electric field. On the other hand, he works in an appropriate distance from carrying current conductors, which are the sources of the magnetic field. The hot-stick workers often operate on the grounded frameworks of metal supports. These metal elements concentrate the electric field in their surroundings. It causes that the electric field strength can exceed in the lineman work zone the admissible value that is determined by appropriate regulations, e.g., European Directive 2004/40/EC [10], concerning the occupational exposure to the electromagnetic fields. This Directive sets action values for time varying and static fields. These action values present levels expressed in values of quantities, which are directly measurable and indicate a threshold above which employers must take one or more of the actions provided for in the Directive. Compliance with these action values will ensure compliance with the relevant exposure limit values. In the case of 50 Hz electric field, the action value is the electric field density of 10 kV/m but the exposure limit value is the current induced in the worker body of the density of 10 mA/m$^2$. These threshold values imposed by the Directive were established on the basis of the recommendations issued by the International Commission on Non-Ionizing Radiation Protection (ICNIRP) [11, 12]. The deadline for transposition of the above-mentioned Directive into the law of the Member States is 30 April 2012.

The aim of this work is to validate a selected numerical technique for the estimation of the electric field in the lineman work zone. Especially, the hot-stick working is here considered. Such a computational field evaluation is very important from the practical point of view because the electric field measurement on the real power object meets some technical difficulties.

A technique that combines the boundary element method (BEM) [13] and a variant of the charge simulation method (CSM) [14, 15] is applied to solve the problem in question. This hybrid technique was earlier successfully employed for the electric field simulation near HV transmission lines and in area of a HV substation [16, 17]; however, in the present issue the field has to be evaluated closer to the elements of tower truss. It can cause a worsening of solution accuracy because the 3D construction elements

are represented by 1D line charges in the approach under consideration.

The author's own software packages has been employed in computations presented in further sections.

## 2. GENERAL ASSUMPTIONS AND NUMERICAL TECHNIQUE

The electric field of energised conductors is disturbed by tower truss elements, insulators, and also by the worker's body. It is well known that the boundary integral techniques are very appropriate to the analysis of open boundary problems, i.e., problems without boundary conditions. Such a problem is here considered. Nevertheless, the application of the BEM to long elements of a relatively small cross-section (angle bars, flat bars, HV line conductors) leads to a large set of algebraic equations and causes a very long solution time.

A variant of the CSM, which is named here the line element method (LEM), can be employed to diminish the size of the matrix equation that has to be solved. In this technique, the live conductors and framework elements are approximated by internally located line charges of unknown values. On the other hand, solid objects like insulators, the human body, etc. are represented by surface charges. It leads to an indirect version of the BEM.

The electric potential at an arbitrary point of the air space is a superposition of the potentials produced by the mentioned line and surface charges. This potential at the surface of the HV line conductor is equal to its phase voltage. The potential is equal to zero at the surface of tower truss elements. The worker's body potential is also equal to zero provided that he stands on or is connected with a grounded object.

Insulators are modelled with dielectric rods of the appropriate electric permittivity. Their surfaces are covered by surface charges representing the dielectric polarisation. The potential of the insulator surface is of unknown value.

When the collocation point, $P_i$, is chosen on the boundary of conductive subregion, the densities of line and surface charges fulfil following Fredholm integral equation of the first kind:

$$\sum_{k=1}^{na} \int_{S_k} G(P, P_i)\sigma(P)\mathrm{d}P + \sum_{l=1}^{nb} \int_{S_l} G(P, P_i)\sigma_f(P)\mathrm{d}P$$

$$+ \sum_{m=1}^{nct} \int_{K_m} G(P, P_i)\tau_f(P)\mathrm{d}P = \varphi(P_i) \tag{1}$$

where:

$na$ — number of insulators.

$nb$ — number of conductive objects modelled with surface charges.

$nc$ — total number of conductive objects modelled with line charges.

$S_k$ — surface of $k$-th insulator.

$S_l$ — surface of $l$-th conductive objects modelled with surface charges.

$K_m$ — curve representing the $m$-th conductor or element of tower truss.

$\sigma(P)$ — surface density of polarisation charge.

$\sigma_f(P)$ — surface density of free charge.

$\tau_f(P)$ — line density of free charge.

$\varphi(P_i)$ — electric potential at the point $P_i$ located on the surface of conducting subregion.

The HV systems of alternating current are considered in the paper; therefore, the potential and charge densities are the complex quantities.

In general, the special fundamental solution for 3D Laplace equation, being antisymmetric with respect to the $xy$ plane is applied in Equation (1) to avoid the ground discretization. This solution is given by the following formula:

$$G(P, P_i) = \frac{1}{4\pi\varepsilon_0}\left(\frac{1}{r_1} - \frac{1}{r_2}\right) \tag{2}$$

where:

$$r_{1,2} = \sqrt{(x - x_i)^2 + (y - y_i)^2 + (z \pm z_i)^2} \tag{3}$$

$\varepsilon_0$ — electric permittivity of surrounding air (electric constant).

The reciprocal of $r_2$ in formula (2) can be neglected when the computation points are located in a long enough distance from the ground plane. In the other words, the simple fundamental solution can be applied in this case. Nevertheless, in the worked out computer program, the special fundamental solution is applied to avoid the computer time consuming procedure, which checks whether the distance is long enough that the influence of the ground could be neglected.

For the collocation point, $P_i$, located on the interface between two dielectrics, the Fredholm integral equation of the second kind can be

formulated:

$$\frac{1}{2\varepsilon_{out}} \frac{\varepsilon_{int} + \varepsilon_{out}}{\varepsilon_{int} - \varepsilon_{out}} \sigma(P_i) + \sum_{k=1}^{na} \int_{S_k} \frac{\partial G(P, P_i)}{\partial n_i} \sigma(P) \mathrm{d}P$$

$$+ \sum_{l=1}^{nb} \int_{S_l} \frac{\partial G(P, P_i)}{\partial n_i} \sigma_f(P) \mathrm{d}P + \sum_{m=1}^{nc} \int_{K_m} \frac{\partial G(P, P_i)}{\partial n_i} \tau_f(P) \mathrm{d}P = 0 \quad (4)$$

$\varepsilon_{int}$ and $\varepsilon_{out}$ denote the electric permittivity of the inner and outer dielectric, respectively. In our case, the inner dielectric represents the insulator and the outer one denotes the air.

The set of two Fredholm integral equations: (1) and (4) forms the basis for the hybrid numerical technique that merges the LEM with BEM. This approach is called further the LEM&BEM. The above set of integral equations is transformed into a set of linear algebraic equations. For this purpose, the HV line conductors as well as frameworks are divided into line elements and similarly surfaces of solid objects into surface elements. The charge densities on these elements are approximated by appropriate functions. The zero-order approximation is applied in the numerical tests and examples presented in the next sections.

After the numerical solution of these equations, the electric field strength at the arbitrary point of the space can be computed using the following formula:

$$E(P_i) = -\sum_{k=1}^{na} \int_{S_k} \mathrm{grad}_i G(P, P_i) \sigma(P) \mathrm{d}P - \sum_{l=1}^{nb} \int_{S_l} \mathrm{grad}_i G(P, P_i) \sigma_f(P) \mathrm{d}P$$

$$- \sum_{m=1}^{nc} \int_{K_m} \mathrm{grad}_i G(P, P_i) \tau_f(P) \mathrm{d}P \quad (5)$$

More details concerning this technique can be find in [16, 17] by the author.

## 3. LEM ERROR ESTIMATION

It is known, e.g., [16, 17], that the considered LEM&BEM approach is sufficiently accurate when the electric field of the HV line is computed near the ground surface, in some distance (about 2 m) from the tower framework that is approximated with the line elements. The analysis of the hot-stick worker exposure requires the electric field evaluation closer to the tower truss. Therefore, to validate an

accuracy of the above method (applied for solving the problem under consideration), the results obtained with the LEM approximation of the tower framework should be compared to the results acquired with a more accurate technique.

A test object of a similar geometry to the geometry of the end part of a HV tower cross-arm is handled for this purpose. The above object consists of a framework (flat and angle bars), insulator and energised conductor of 200 kV.
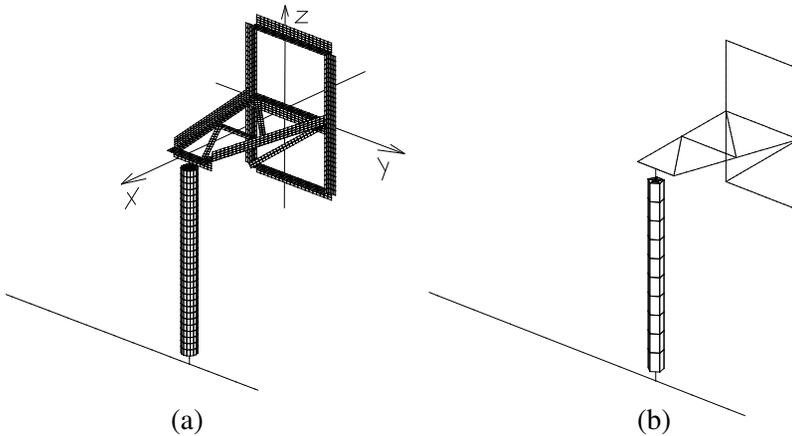


(a)                                                    (b)

**Figure 2.** Models of the test object. (a) Detailed approximation. (b) Crude approximation.
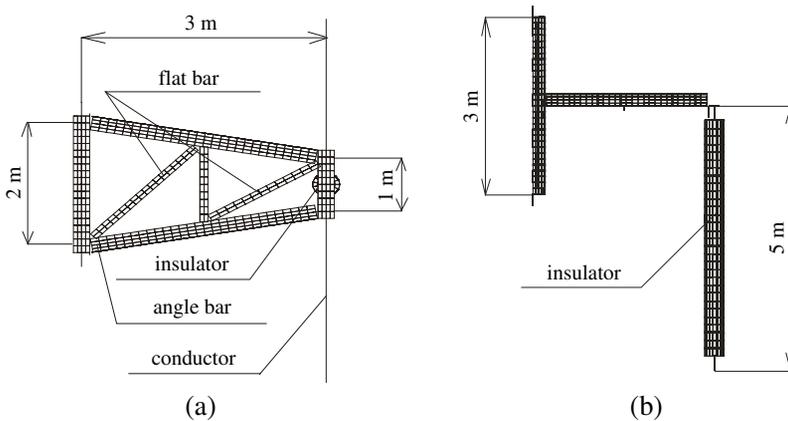


(a)                                                    (b)

**Figure 3.** Detailed model of the test object. (a) Horizontal projection. (b) Vertical projection.

The flat bars transverse dimension is $0.1\,\mathrm{m}$ but the angle bars cross-sections are $0.2\,\mathrm{m} \times 0.2\,\mathrm{m}$ and $0.1\,\mathrm{m} \times 0.1\,\mathrm{m}$. Such shapes are frequently used as structural elements of cross-arms of $400\,\mathrm{kV}$ towers.

The detailed and crude approximation of this object is exhibited in Figure 2. In the crude approximation, the framework angle and flat bars are substituted by the line elements but in the detailed one the framework is represented by the boundary elements. In the both models the insulator is approximated with the boundary elements and the energised conductor with the line elements. The first model presents the LEM&BEM approach that was outlined in the previous section but the second one is named here the detailed LEM&BEM.

The overall dimensions of the object under consideration are exhibited in Figure 3. The detailed model is subdivided into $2235$ boundary elements (framework, insulator) and $45$ line elements (conductor). On the other hand, simplified model is approximated with $60$ boundary elements (insulator) and $135$ line elements (conductor, framework).

Computational results of the electric field distribution obtained for the above described two numerical models of the test object are presented in Figures 4 and 5. The computations have been performed along the axis $x$, for $y = 0$ and for four different levels over the cross-arm, namely for $z$ equal to: $0.25\,\mathrm{m}$, $0.5\,\mathrm{m}$, $0.75\,\mathrm{m}$, and $1\,\mathrm{m}$.

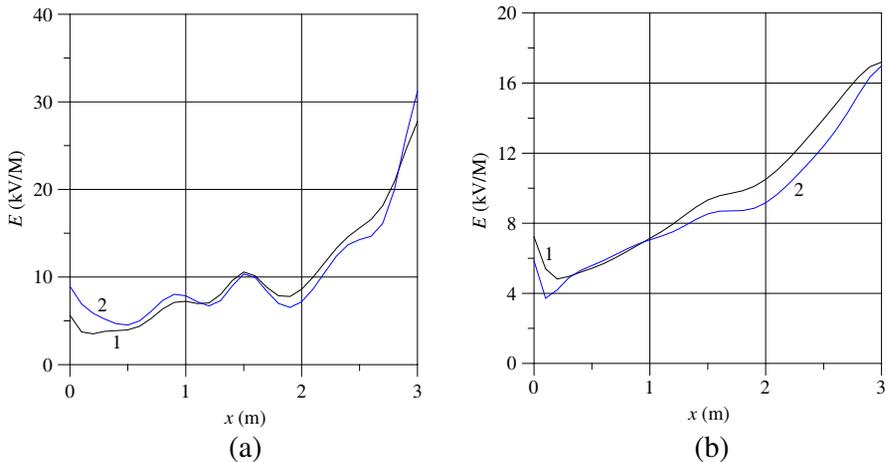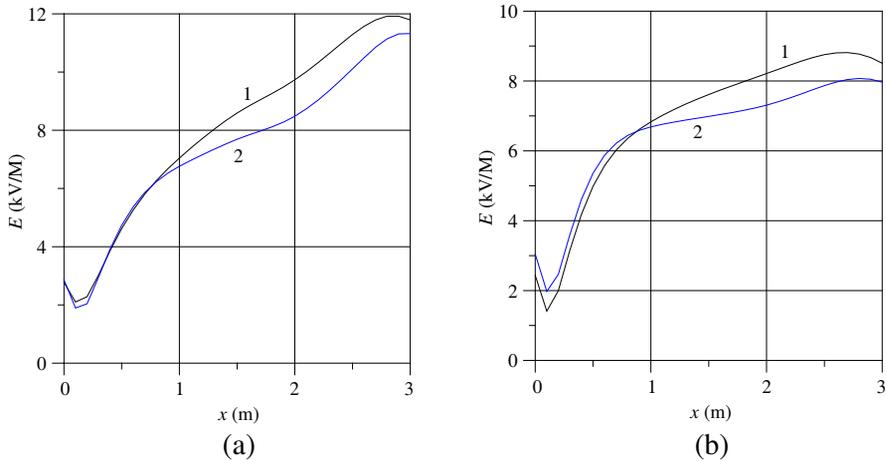Obviously, some discrepancy between results obtained using these



**Figure 4.** Electric field distribution near the detailed (1) and crude (2) model of the test object for $y = 0$, along $x$ axis. (a) $z = 0.25\,\mathrm{m}$, (b) $z = 0.5\,\mathrm{m}$.

**Figure 5.** Electric field distribution near the detailed (1) and crude (2) model of the test object for $y = 0$, along $x$ axis. (a) $z = 0.75\,\mathrm{m}$, (b) $z = 1\,\mathrm{m}$.

two numerical models can be observed in Figures 4 and 5. Nevertheless, the crude approach has very important advantages in compare with the detailed one. The pre-processing is much simpler in this case and the solution time is significantly shorter.

The total solution time on a Intel Core 2 Duo, T7600, 2.33 GHz computer with 4 GB RAM is about 12 minutes for the detailed object approximation and 2 second for the crude one. The above solution times include the time of object subdivision, calculation of coefficients of equation system, solution of equation system and calculating of the electric field strength at the considered points of space.

Taking into account, that the numerical model of the real object needs much more elements than the test object model, one can state that the proposed LEM&BEM technique can be an useful tool for the first estimation of the electric field exposure during the live-line works on power objects.

## 4. GEOMETRY OF THE HUMAN BODY MODEL

The action value (10 kV/m), set in European Directive 2004/40/EC [10], is referred to the strength of the electric field that is undisturbed by the worker's body. Nevertheless, the estimation of the electric field concentrated around the human body is useful for dosimetry studies as well as for evaluation of currents (exposure limit values) induced

in human body due to the electric field. An axisymmetric numerical model of the human body is employed in the present paper. This model is recommended by the appropriate IEC/EN standards, e.g., IEC/EN 62233 [18], for the evaluation of the currents induced in the human body due to the external magnetic fields. In the present paper, the model considered is validated in the context of the electric field exposure. Basic dimensions of this model are presented in Figure 6, where a subdivision of its boundary is also exhibited.
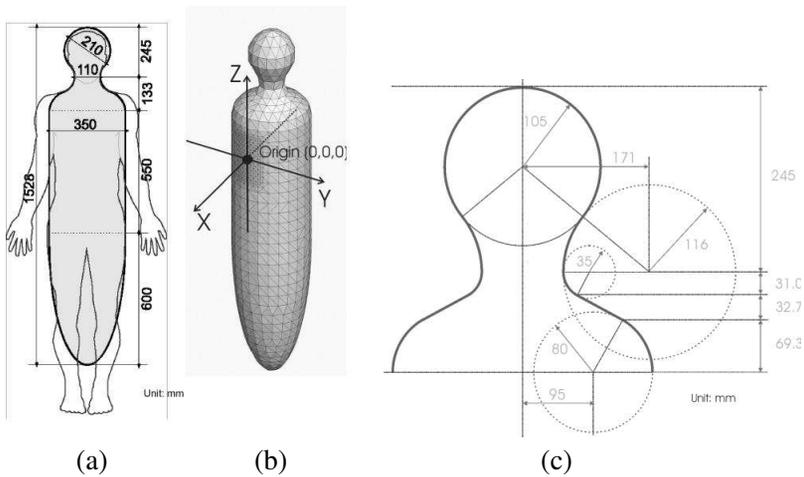


**Figure 6.** Numerical model of the human body. (a) Basic dimensions. (b) Surface subdivision. (c) Detailed dimensions of the head and shoulders.
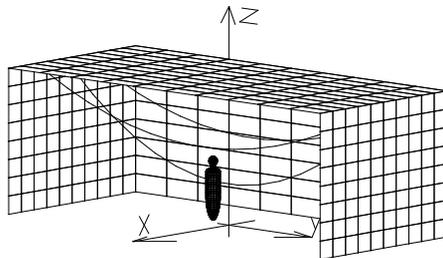


**Figure 7.** Numerical model of the laboratory room with suspended cables and the human body model.

## 5. MEASUREMENTS OF THE ELECTRIC FIELD NEAR THE HUMAN BODY

Measurement results taken in a laboratory are presented in this section to validate the utility of the considered body model for the analysis of the human exposure to the electric field.

The laboratory was located in a room of dimensions: $10\,\text{m} \times 4.6\,\text{m} \times 3.5\,\text{m}$. A model of a transmission line was located in this room. The above model consists of three cables suspended as it is shown in Figures 7 and 8. The conductors are connected to a three-phase
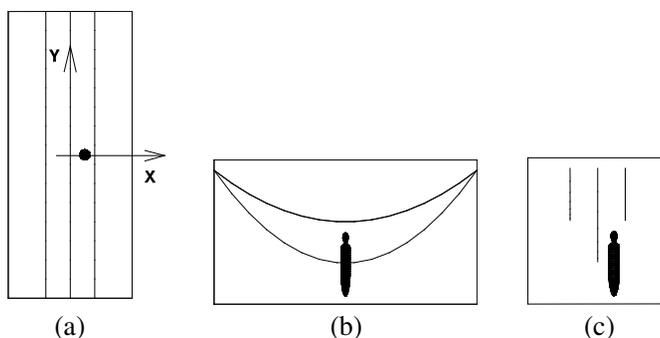


(a)                    (b)                    (c)

**Figure 8.** Sketch of the laboratory room with suspended cables and the human body model. (a) Horizontal projection. (b) and (c) Vertical projections.
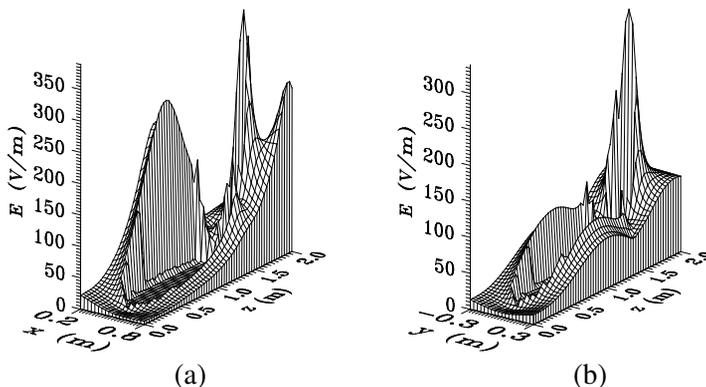


(a)                                    (b)

**Figure 9.** Computed electric field distribution around the model of human body that is located near the laboratory model of the transmission line. (a) For $y = 0$. (b) For $x = 0.53\,\text{m}$.

autotransformer of a low voltage. The measurements were made with an integrated meter of the electric and magnetic fields Maschek ESM-100 (manufactured by Maschek Elektronik, Germany). Its maximum error is ±5%.

During measurements the height of cable suspension was 3.25 m and the clearance between them was 0.6 m. The minimum cable distance to the floor was: 1 m for the central cable and 2 m for the outer ones. The cable phase voltage was 225 V.

The electric field has been measured in surroundings of a real man of dimensions approximate the body model. The man was situated between the cables as it is shown in Figure 8. Co-ordinates of the man's vertical axis was: $x = 53$, $y = 0$.

For comparison, the electric field distribution in the vicinity of the numerical body model has been computed. These numerical results are exhibited in Figure 9.

The measurement results as well as the results of computations, at the chosen points in the distance of 0.03 m from the human body, are presented in Tables 1 and 2. A satisfactory convergence of the above

**Table 1.** Computational and measurement results of the electric field strength around the model of human body near the laboratory model of transmission line (phase voltage 225 V, $y = 0$).

| Part of body | $x$ | $z$ | $E$ calculated | $E$ measured |
|---|---|---|---|---|
| - | m | m | V/m | V/m |
| Over head | 0.530 | 1.755 | 353.0 | 335 |
| Head | 0.395 | 1.725 | 74.4 | 66 |
| Head | 0.665 | 1.725 | 236.1 | 237 |
| Neck | 0.445 | 1.52 | 36.3 | 26 |
| Neck | 0.615 | 1.52 | 88.5 | 80.5 |
| Shoulder | 0.325 | 1.42 | 95.8 | 150 |
| Shoulder | 0.735 | 1.42 | 117.4 | 120 |
| Elbow | 0.325 | 1.10 | 267.5 | 235 |
| Elbow | 0.735 | 1.10 | 49.8 | 40.0 |
| Hip | 0.325 | 0.92 | 268.7 | 259 |
| Hip | 0.735 | 0.92 | 34.0 | 29.0 |
| Knee | 0.33 | 0.50 | 86.0 | 92.0 |
| Knee | 0.73 | 0.50 | 15.1 | 11.0 |

**Table 2.** Computational and measurement results of the electric field strength around the model of human body near the laboratory model of transmission line (phase voltage $U = 225\,\text{V}$, $x = 0.53$).

| Part of body | $y$ | $z$ | $E$ calculated | $E$ measured |
|:---:|:---:|:---:|:---:|:---:|
| - | m | m | V/m | V/m |
| Head | 0.135 | 1.725 | 151.5 | 145 |
| Head | −0.135 | 1.725 | 151.5 | - |
| Neck | 0.085 | 1.52 | 52.5 | 44.5 |
| Neck | −0.085 | 1.52 | 52.5 | - |
| Shoulder | 0.205 | 1.42 | 70.3 | 75.0 |
| Shoulder | −0.205 | 1.42 | 70.3 | - |
| Elbow | 0.205 | 1.10 | 91.6 | 90.0 |
| Elbow | −0.205 | 1.10 | 91.6 | - |
| Hip | 0.205 | 0.92 | 92.8 | 80.0 |
| Hip | −0.205 | 0.92 | 92.8 | - |
| Knee | 0.205 | 0.50 | 45.4 | 35 |
| Knee | −0.205 | 0.50 | 45.4 | - |

results can be observed at the majority of considered points. The major discrepancy appears near the left shoulder (from the side of the central cable). Simplification of the body model that is without the limbs can account for this discrepancy. Generally, the above simplification can be accepted because the regulations concerning the occupational exposure to the electromagnetic fields are related to the head and trunk only. Nevertheless, the above simplification can cause the local computational errors.

## 6. MEASUREMENTS ON A REAL STRAIGHT-LINE TOWER OF 400 KV

In this section, the results of measurements of the electric field distribution in the working zone of hot-stick workers are compared to the results of calculations for a further estimation of the applied numerical technique.

Experimental results of the electric field strength within a cross-arm of a real 400 kV straight-line tower (shown in Figure 10(a)) have been published in [19].

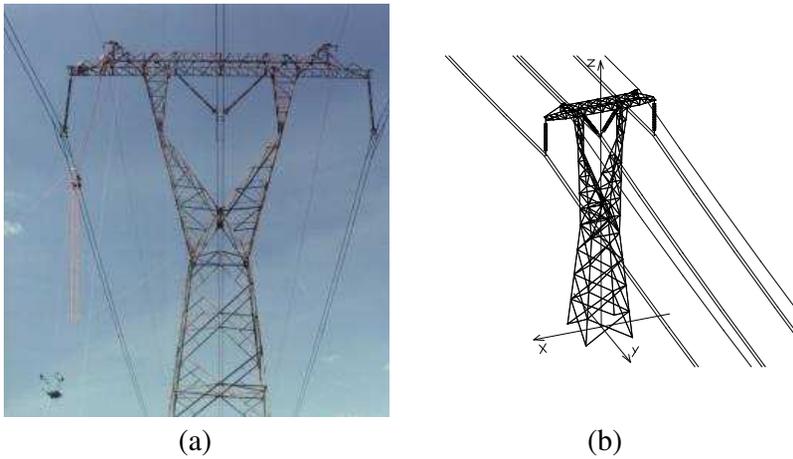A numerical model of this tower that consists of 826 line elements

**Figure 10.** (a) Straight-line tower of $400\,\text{kV}$ and (b) its numerical model.
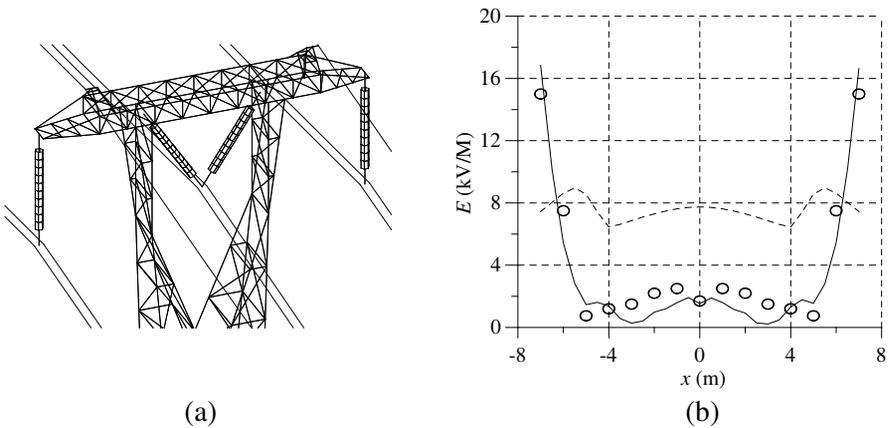


**Figure 11.** (a) Cross-arm of the $400\,\text{kV}$ tower and (b) the electric field within this cross-arm. Continuous line — computations (influence of the tower truss is taken into account). Dash line — computations (influence of the tower truss is neglected). Circles — measurements on the real object.

and 180 boundary elements (insulators) is exhibited in Figures 10(b) and 11(a). This line-element mesh is generated automatically by the own author's program BEMsolver 3D.

The computational as well as measurement results of the electric field strength are plotted in Figure 11(b). In this figure, co-ordinate $x$ denotes a distance from the tower axis.

The good convergence of these results can be observed in the end part of the cross-arm, where the field strength reaches the greatest values. The convergence is worse in the middle part of the cross-arm, where the electric field strength is much smaller. In this region, it is shielded effectively by the tower framework. The computational results of the electric field distribution within the cross-arm when the tower truss influence is neglected is presented in the above figure, as well. It shows that the tower framework should be taken into account in computations indispensably.

## 7. HOT-STICKS WORKERS EXPOSURE ON 400 KV ANCHOR TOWER

Computational results of the electric field in the live-line-working zone (over the end of the cross-arm of the 400 kV anchor tower shown in Figure 12(a)) has been presented in this section. The approximation of this tower by the line elements is exhibited in Figures 12(b) and 13(a). The numerical model of worker's body is also shown in these figures.

The electric field distribution affected by the tower truss as well as worker's body is plotted in Figure 13(b). Its strength reaches 100 kV/m in the considered domain.

The strength of the electric field that is undisturbed by the human body is more interesting for the estimation of the worker's exposure. This field distribution is presented in Figure 14(a). It reaches locally 20 kV/m in this case.

According to European Directive 2004/40/EC workers should not be exposed to the electric field of the strength higher than 10 kV/m.
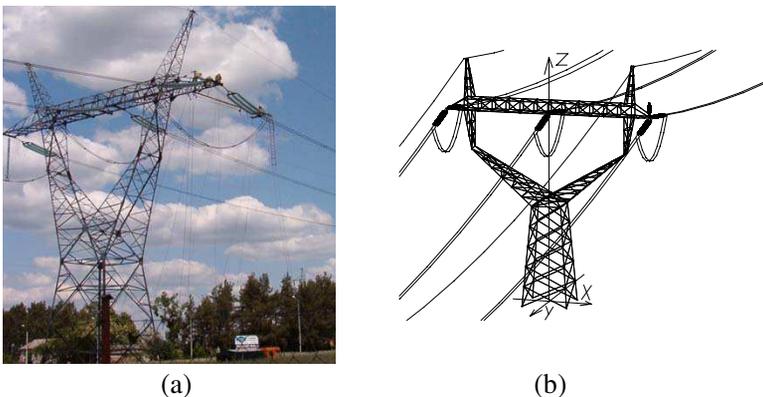


(a) (b)

**Figure 12.** (a) Anchor tower of the 400 kV transmission line and (b) its numerical model.
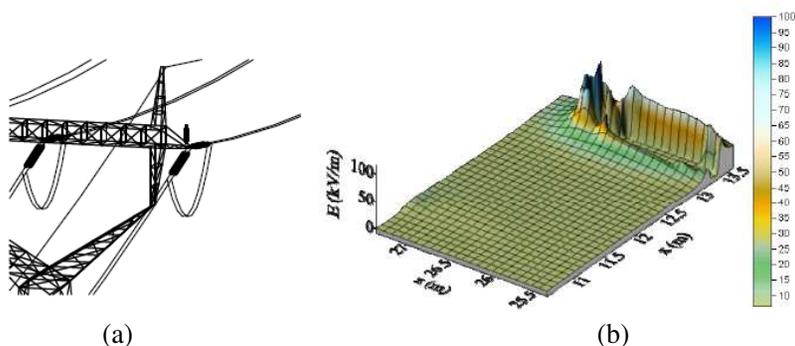
**Figure 13.** (a) Numerical model of the hot-stick worker on the cross-arm model of the 400 kV anchor tower. (b) The electric field distribution around the worker's body.
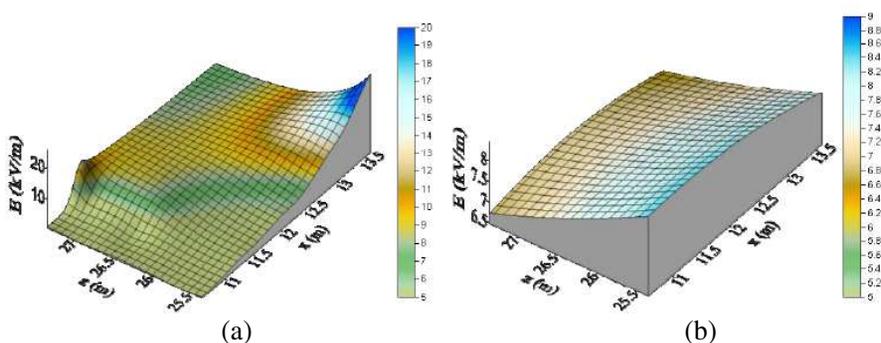


**Figure 14.** Electric field distribution over the end of cross-arm of the 400 kV anchor tower. (a) Influence of tower truss is taken into account. (b) Influence of tower truss is neglected.

Polish regulations admit the occupational exposure to the electric field of the strength greater than 10 kV/m provided that the appropriate field dose is not exceeded. This dose is described by formula: $D_E = E^2 t$, where $E$ is the electric field strength in the working zone and $t$ is the exposure time, $t \leq 8$ h. The real field dose cannot transgress the value of the admissible dose that is: $Dd_E = 800 \, (\text{kV/m})^2 \times$ h for $10 \, \text{kV/m} < E < 20 \, \text{kV/m}$.

For comparison, the distribution of the undisturbed (by the human body and tower framework) electric field over the end part of the cross-arm under consideration is exhibited in Figure 14(b). The last results indicate falsely that the electric field strength does not reach 10 kV/m

in the working zone. It shows once again that the tower truss influence should be taken into account in computations for the proper estimation of worker's exposure to the electric field.

## 8. CONCLUSION

The utility of the proposed simplified boundary integral approach (called in the paper the LEM&BEM) for the analysis of the electric field in the lineman working zone has been validated. The test object similar to the end of the tower cross-arm has been handled for this purpose. The results obtained with the LEM&BEM model of the test object has been compared to these obtained with detailed LEM&BEM approach.

The simplified model of the whole tower framework has been also analysed. The numerical results that are obtained employing this model have been compared to the measurements taken on the real tower of the 400 kV transmission line.

Sufficient convergence of the above results corroborates the effectiveness of the proposed computational technique for the first estimation of the live-line-worker exposure to the electric field.

Moreover, the simplified numerical human body model for the analysis of the electric field around the live-line worker has been examined in the paper. The numerical results have been compared to the measurement ones taken in the laboratory. The satisfactory convergence of these results confirms the utility of this model for future estimation of the currents induced in the human body due to external electric fields.

The numerical analysis of the electric field distribution in the hot-stick-working zone on the anchor tower of the 400 kV transmission line is presented to demonstrate the efficiency of the numerical technique under consideration.

## REFERENCES

1. Stuchly, M. A. and S. Zhao, "Magnetic field-induced currents in human body in proximity of power lines," *IEEE Trans. on Power Delivery*, Vol. 11, No. 1, 102–108, 1996.

2. Dawson, T. W., K. Caputa, and M. Stuchly, "Magnetic field exposure for UK live-line workers," *Physics in Medicine and Biology*, No. 47, 995–1012, 2002.

3. Cherubini, E., N. Chavannes, and N. Kuster, "Realistic skeleton based deformation of high-resolution anatomical human models

for electromagnetic simulation," *The 31st Annual Meeting of the Bioelectromagnetic Society*, 2009.

4. Hirata, A., H. Sugiyama, and O. Fujiwara, "Estimation of core temperature elevation in humans and animals for whole-body averaged SAR," *Progress In Electromagnetics Research*, Vol. 99, 53–70, 2009.

5. Chou, H.-H., H.-T. Hsu, H.-T. Chou, K.-H. Liu, and F.-Y. Kuo, "Reduction of peak SAR in human head for handset applications with resistive sheets (r-cards)," *Progress In Electromagnetics Research*, Vol. 94, 281–296, 2009.

6. Gemio, J., J. Parron, and J. Soler, "Human body effects on implantable antennas for ism bands applications: models comparison and propagation losses study," *Progress In Electromagnetics Research*, Vol. 110, 437–452, 2010.

7. Sabbah, A. I., N. I. Dib, and M. A. Al-Nimr, "SAR and temperature elevation in a multi-layered human head model due to an obliquely incident plane wave," *Progress In Electromagnetics Research M*, Vol. 13, 95–108, 2010.

8. Krajewski, W., "Numerical assessment of electromagnetic exposure during live-line works on high-voltage objects," *IEE Proc. Science, Measurement and Technology*, Vol. 3, No. 1, 27–38, 2009.

9. Krajewski, W., "Numerical evaluation of the magnetic field exposure near the transition tower of an overhead-underground HV line," *Progress In Electromagnetics Research M*, Vol. 14, 247–261, 2010.

10. "Directive 2004/40/EC of the European Parliament and of the Council of 29 April 2004 on the minimum health and safety requirements regarding the exposure of workers to the risk arising from physical agents (electromagnetic fields) (18th individual Directive within the meaning of Article 16 (1) of Directive 89/391/EEC)," *Official Journal of the European Union*, Nr L-184, 1–9, 2004.

11. International Commission on Non-Ionizing Radiation Protection (ICNIRP), "Guidelines for limiting exposure to time-varying electric, magnetic, and electromagnetic fields (up to 300 GHz)," *Health Physics*, Vol. 74, No. 4, 494–522, 1998.

12. International Commission on Non-Ionizing Radiation Protection (ICNIRP), "Guidelines for limiting exposure to time-varying electric and magnetic fields (1 Hz to 100 kHz)," *Health Physics*, Vol. 99, No. 6, 818–836, 2010.

13. Brebbia, C. A., J. C. F. Telles, and L. C. Wrobel, *Boundary Element Techniques*, Springer, Berlin, Heidelberg, New York, 1984.

14. Singer, H., H. Steinbigler, and P. Weiss, "A charge simulation method for the calculation of high voltage fields," *IEEE Trans. on Power Apparatus and Systems*, Vol. 93, 1660–1668, 1973.

15. Ranković, A. and M. S. Savić, "Generalized charge simulation method for the calculation of the electric field in high voltage substations," *Electrical Engineering (Archiv fur Elektrotechnik)*, Vol. 92, No. 2, 69–77, 2010.

16. Krajewski, W., "Boundary and line elements in the analysis of selected EMC problems of low frequency," *Prace Instytut Elektrotechniki (Proceedings of Electrotechnical Institute)*, Zeszyt 224, 2005 (Monograph in Polish).

17. Krajewski, W., "Numerical modelling of the electric field in HV substations," *IEE Proc. Science, Measurement and Technology*, Vol. 151, No. 4, 267–272, 2004.

18. IEC/EN 62233, "Measurement methods for electromagnetic fields of household appliances and similar apparatus with regard to human exposure," International Electrotechnical Commission, Geneva, 2005.

19. Łopatkiewicz, R., Z. Nadolny, and A. Rakowska, "Analysis of electric field intensity during live maintenance on 400 kV overhead power transmission line," *Przagląd Elektrotechniczny (Electrical Review)*, No. 11b, 258–261, 2010 (in Polish).